

Revisiting NARX Recurrent Neural Networks for Long-Term Dependencies

Robert DiPietro¹ Nassir Navab^{1,2} Gregory D. Hager^{1,3}

Abstract

Recurrent neural networks (RNNs) have shown success for many sequence-modeling tasks, but learning long-term dependencies from data remains difficult. This is often attributed to the *vanishing gradient problem*, which shows that gradient components relating a loss at time t to time $t - \tau$ tend to decay exponentially with τ .

Long short-term memory (LSTM) and gated recurrent units (GRUs), the most widely-used RNN architectures, attempt to remedy this problem by making the decay's *base* closer to 1. NARX RNNs¹ take an orthogonal approach: by including direct connections, or *delays*, from the past, NARX RNNs make the decay's *exponent* closer to 0. However, as introduced, NARX RNNs reduce the decay's exponent only by a factor of n_d , the number of delays, and simultaneously increase computation by this same factor.

We introduce a new variant of NARX RNNs, called MIXed hiSTory RNNs, which addresses these drawbacks. We show that for $\tau \leq 2^{n_d-1}$, MIST RNNs reduce the decay's worst-case exponent from τ/n_d to $\log \tau$, while maintaining computational complexity that is similar to LSTM and GRUs. We compare MIST RNNs to simple RNNs, LSTM, and GRUs across 4 diverse tasks. MIST RNNs outperform all other methods in 2 cases, and in all cases are competitive.

1. Introduction

Recurrent neural networks (Rumelhart et al., 1986; Werbos, 1988; Williams & Zipser, 1989) are a powerful class of neural networks that are naturally suited to modeling time series data and other sequential data. For example,

¹Johns Hopkins University, USA. ²Technische Universität München, Germany. ³Institute for Advanced Study at Technische Universität München, Germany. Correspondence to: Robert DiPietro <rdipietro@gmail.com>.

¹The acronym NARX stems from Nonlinear AutoRegressive models with eXogenous inputs.

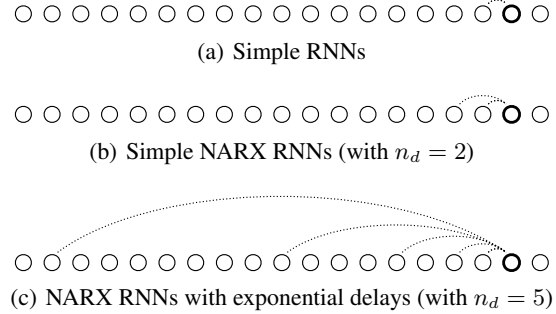


Figure 1. Direct connections from the past to a single time step t for various architectures. NARX RNNs allow the number of delays n_d to exceed 1.

in recent years alone, RNNs have achieved state-of-the-art performance on tasks as diverse as speech recognition (Miao et al., 2015), generative image modeling (Oord et al., 2016), and machine translation (Wu et al., 2016).

However, despite their success, RNNs remain difficult to train, and it is especially difficult for RNNs to learn long-term dependencies from data. This difficulty is often attributed to the *vanishing gradient problem* (Hochreiter, 1991; Bengio et al., 1994; Pascanu et al., 2013), which shows that gradient components relating a loss at time t to events at time $t - \tau$ tend to either explode or vanish exponentially. The problem of exploding gradients is often remedied in practice with simple heuristics such as gradient clipping, but overcoming the problem of vanishing gradients has proven much more difficult.

The vanishing gradient problem is illustrated in Figures 1 and 2. Figure 1 shows connections for a single time step. These connections are replicated across all time steps, forming paths from $t - \tau$ to t , and each path yields a gradient component that can be expressed as a product of factors, one factor per edge. This can be seen in Figure 2, which shows some *shortest* paths. If we denote the maximum spectral norm of any such factor as λ , then the norm of the product is upper bounded by λ^{n_e} , where n_e is the number of edges along the path. Therefore when $\lambda < 1$, events at $t - \tau$ with large τ have nearly no effect on gradients, making it extremely difficult to learn from these events.

Simple RNNs (Elman, 1990) are especially vulnerable to

this problem, whereas long short-term memory (Hochreiter & Schmidhuber, 1997; Gers et al., 2000), gated recurrent units (Cho et al., 2014), and NARX RNNs (Lin et al., 1996) are all less vulnerable. LSTM and GRUs introduce gating mechanisms which create paths that increase the base λ to be closer to 1. In contrast, NARX RNNs introduce delays from the distant past, creating paths that decrease the exponent n_e . As introduced, however, NARX RNNs suffer from two major drawbacks. First, they reduce the exponent n_e only by a factor of n_d , the number of delays; second, they increase computation by this same factor, which severely inhibits their use in practice.

In this work, we introduce a new variant of NARX RNNs, called MIXed hiSTory RNNs, or MIST RNNs, which resolves both of these issues. First, by using exponential delays rather than continuous delays, then for $\tau \leq 2^{n_d-1}$, the worst-case exponent n_e is reduced from τ/n_d to $\log \tau$. Second, by restricting ourselves to a (learned) convex combination of previous states, we maintain a computational complexity that is similar to LSTM and GRUs.

In the next section, we describe background material and related work. In Section 3, we move on to the vanishing gradient problem in the context of NARX RNNs; here, we derive the gradient decomposition that is stated in (Bengio et al., 1994; Pascanu et al., 2013) from first principles, and we simultaneously extend this derivation to NARX RNNs. This motivates MIST RNNs, which we describe next. In Section 5, we perform an extensive set of experiments across 4 diverse tasks comparing simple RNNs, LSTM, GRUs, and MIST RNNs, and finally in Section 6 we conclude and describe directions for future work.

2. Background and Related Work

Recurrent neural networks, as commonly described in literature, take on the general form

$$\mathbf{h}_t = f(\mathbf{h}_{t-1}, \mathbf{x}_t, \boldsymbol{\theta}) \quad (1)$$

which compute a new state² \mathbf{h}_t in terms of the previous state \mathbf{h}_{t-1} , the current input \mathbf{x}_t , and some parameters $\boldsymbol{\theta}$ (which are shared over time).

One of the earliest variants, now known to be especially vulnerable to the vanishing gradient problem, is that of simple RNNs (Elman, 1990), described by

$$\mathbf{h}_t = \tanh(\mathbf{W}_h \mathbf{h}_{t-1} + \mathbf{W}_x \mathbf{x}_t + \mathbf{b}) \quad (2)$$

In this equation and elsewhere in this work, all weight matrices \mathbf{W} and biases \mathbf{b} collectively form the parameters $\boldsymbol{\theta}$

²In this work, we use \mathbf{h}_t for consistency, but to avoid any confusion, we note that not all of \mathbf{h}_t needs be exposed externally. Notable examples are LSTM and RNNs with multiple layers.

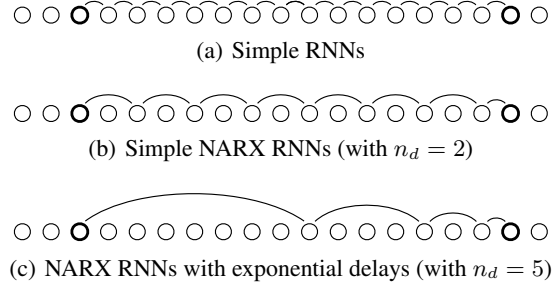


Figure 2. Shortest paths connecting time $t - \tau$ to time t , here with $\tau = 15$. Information flows forward along these paths for predictions and backward along these paths for gradients, but can be destroyed by the multiplicative factors encountered at each edge.

to be learned, and \tanh is always written explicitly³.

Long short-term memory (Hochreiter & Schmidhuber, 1997; Gers et al., 2000), the most widely-used RNN architecture to date, was introduced specifically to address the vanishing gradient problem. In LSTM, the vanishing gradient problem is mitigated through a nearly-additive path among adjacent memory cells.

A recently-proposed architecture, inspired by LSTM, is that of gated recurrent units (Cho et al., 2014). GRUs are simpler than LSTM, as they use one less gate and eliminate the need for distinguishing between hidden states and memory cells, and are described by

$$\mathbf{r}_t = \sigma(\mathbf{W}_{rh} \mathbf{h}_{t-1} + \mathbf{W}_{rx} \mathbf{x}_t + \mathbf{b}_r) \quad (3)$$

$$\mathbf{u}_t = \sigma(\mathbf{W}_{uh} \mathbf{h}_{t-1} + \mathbf{W}_{ux} \mathbf{x}_t + \mathbf{b}_u) \quad (4)$$

$$\tilde{\mathbf{h}}_t = \tanh(\mathbf{W}_h [\mathbf{r}_t \odot \mathbf{h}_{t-1}] + \mathbf{W}_x \mathbf{x}_t + \mathbf{b}) \quad (5)$$

$$\mathbf{h}_t = \mathbf{u}_t \odot \mathbf{h}_{t-1} + (\mathbf{1} - \mathbf{u}_t) \odot \tilde{\mathbf{h}}_t \quad (6)$$

where $\sigma(\cdot)$ denotes the element-wise sigmoid function and \odot denotes element-wise multiplication. GRUs mitigate the vanishing gradient problem using a mechanism very similar to that of LSTM; from Equation 6, we can see that if $u_{t,i}$ is nearly 1, then the corresponding derivative $\frac{\partial h_{t,i}}{\partial h_{t-1,i}}$ is also nearly 1. \mathbf{r}_t and \mathbf{u}_t are referred to as the reset and update gates. We describe GRUs in detail here because MIST RNNs will adopt reset gates from GRUs.

NARX RNNs (Lin et al., 1996) also address the vanishing gradient problem, but using a mechanism that is orthogonal to (and possibly complementary to) that of LSTM and GRUs. This is done by allowing *delays*, or direct connections from the past. NARX RNNs in their general form are described by

$$\mathbf{h}_t = f(\mathbf{h}_{t-1}, \mathbf{h}_{t-2}, \dots, \mathbf{x}_t, \mathbf{x}_{t-1}, \dots, \boldsymbol{\theta}) \quad (7)$$

³ \tanh is a common choice, but it is of course also possible to use other activation functions.

but literature usually describes the specific variant explored in (Lin et al., 1996),

$$\mathbf{h}_t = \tanh \left(\left[\sum_{d=1}^{n_d} \mathbf{W}_d \mathbf{h}_{t-d} \right] + \mathbf{W}_x \mathbf{x}_t + \mathbf{b} \right) \quad (8)$$

We will refer to this variant as *simple* NARX RNNs. From an efficiency perspective, notice that if the dimensionality of \mathbf{h}_t is similar to or greater than that of \mathbf{x}_t , as is often the case in practice, then a simple NARX RNN has approximately n_d times as many parameters and requires approximately n_d times as much computation as its corresponding simple RNN (with $n_d = 1$).

Finally we remark that many other approaches have also been proposed to capture long-term dependencies. One recent idea that is related to this work is that of attention (Bahdanau et al., 2015), which also forms convex combinations over previous states. However, attention mechanisms differ in two major ways. First, the combinations are *external*, in that RNN states themselves are not combinations of previous states. Second, attention mechanisms typically combine all previous states, leading to a complexity that is quadratic in sequence length (rather than linear). Other notable approaches include Hessian-free optimization (Martens & Sutskever, 2011), operating explicitly at multiple time scales (El Hahi & Bengio, 1995; Koutnik et al., 2014), using associative or explicit memory (Plate, 1993; Danihelka et al., 2016; Graves et al., 2014; Weston et al., 2015; Sukhbaatar et al., 2015), and initializing or restricting weight matrices to be orthogonal (Arjovsky et al., 2016; Henaff et al., 2016).

3. The Vanishing Gradient Problem in the Context of NARX RNNs

Here we use *chain rule for ordered derivatives* (Werbos, 1990) to derive the gradient decomposition stated in (Bengio et al., 1994; Pascanu et al., 2013) for RNNs, and to simultaneously generalize the result to NARX RNNs. Since the chain rule for ordered derivatives is easily derived from the standard chain rule (Werbos, 1989), it is easily accessible to all, and solidifies intuitions that are based on the backpropagation-through-time algorithm.

3.1. Disambiguating Notation

First, to avoid confusion, we disambiguate the symbol $\frac{\partial \mathbf{f}}{\partial \mathbf{x}}$, which is routinely overloaded in literature. We illustrate this by example. Consider the Jacobian of $\mathbf{f}(\mathbf{u}(\mathbf{x}), \mathbf{v}(\mathbf{x}))$ with respect to \mathbf{x} ; from the ordinary chain rule, we have $\frac{\partial \mathbf{f}}{\partial \mathbf{x}} = \frac{\partial \mathbf{f}}{\partial \mathbf{u}} \frac{\partial \mathbf{u}}{\partial \mathbf{x}} + \frac{\partial \mathbf{f}}{\partial \mathbf{v}} \frac{\partial \mathbf{v}}{\partial \mathbf{x}}$. Next, consider the Jacobian of $\mathbf{f}(\mathbf{x}, \mathbf{u}(\mathbf{x}))$; from a naive application of the chain rule, we obtain $\frac{\partial \mathbf{f}}{\partial \mathbf{x}} = \frac{\partial \mathbf{f}}{\partial \mathbf{x}} \frac{\partial \mathbf{x}}{\partial \mathbf{x}} + \frac{\partial \mathbf{f}}{\partial \mathbf{u}} \frac{\partial \mathbf{u}}{\partial \mathbf{x}}$, which is clearly incorrect. The problem is that on the left $\frac{\partial \mathbf{f}}{\partial \mathbf{x}}$ denotes $\frac{\partial \mathbf{f}(\mathbf{x})}{\partial \mathbf{x}}$, a collection of

full derivatives, whereas on the right $\frac{\partial \mathbf{f}}{\partial \mathbf{x}}$ denotes $\frac{\partial \mathbf{f}(\mathbf{x}, \mathbf{u})}{\partial \mathbf{x}}$, a collection of partial derivatives.

In this work, we denote full derivatives with $\frac{\partial^+ \mathbf{f}}{\partial \mathbf{x}}$ and partial derivatives with $\frac{\partial \mathbf{f}}{\partial \mathbf{x}}$, for example letting us express $\frac{\partial^+ \mathbf{f}}{\partial \mathbf{x}}$ above as $\frac{\partial^+ \mathbf{f}}{\partial \mathbf{x}} = \frac{\partial \mathbf{f}}{\partial \mathbf{x}} \frac{\partial^+ \mathbf{x}}{\partial \mathbf{x}} + \frac{\partial \mathbf{f}}{\partial \mathbf{u}} \frac{\partial^+ \mathbf{u}}{\partial \mathbf{x}}$. We note that this notation is consistent with (Werbos, 1989; 1990), but is the exact opposite of the convention in (Pascanu et al., 2013).

3.2. The Chain Rule for Ordered Derivatives

Consider an ordered system of n vectors $\mathbf{v}_1, \mathbf{v}_2, \dots, \mathbf{v}_n$, where each is expressed as a function of all previous vectors:

$$\mathbf{v}_i \equiv \mathbf{v}_i(\mathbf{v}_{i-1}, \mathbf{v}_{i-2}, \dots, \mathbf{v}_1), \quad 1 \leq i \leq n \quad (9)$$

The chain rule for ordered derivatives expresses the full derivatives $\frac{\partial^+ \mathbf{v}_i}{\partial \mathbf{v}_j}$ for any $j < i$ in terms of the full derivatives⁴ that relate \mathbf{v}_i to all previous \mathbf{v}_k :

$$\frac{\partial^+ \mathbf{v}_i}{\partial \mathbf{v}_j} = \sum_{i \geq k > j} \frac{\partial^+ \mathbf{v}_i}{\partial \mathbf{v}_k} \frac{\partial \mathbf{v}_k}{\partial \mathbf{v}_j}, \quad j < i \quad (10)$$

3.3. Temporal Decomposition

Now consider NARX RNNs in their general form (Equation 7), and for simplicity⁵ consider the situation that is most often encountered in practice, where the loss at time t is defined in terms of the current state \mathbf{h}_t and its own parameters θ_l (which are independent of θ):

$$l_t = f_l(\mathbf{h}_t, \theta_l) \quad (11)$$

Then the Jacobian (or transposed gradient) with respect to θ can be written as

$$\frac{\partial^+ l_t}{\partial \theta} = \frac{\partial f_l}{\partial \mathbf{h}_t} \frac{\partial^+ \mathbf{h}_t}{\partial \theta} \quad (12)$$

because the additional term $\frac{\partial f_l}{\partial \theta_l} \frac{\partial^+ \theta_l}{\partial \theta}$ is $\mathbf{0}$. Now, by letting $\mathbf{v}_1 = \theta$, $\mathbf{v}_2 = \mathbf{x}_1$, $\mathbf{v}_3 = \mathbf{x}_2$, and so on in Equations 9 and 10, we obtain

$$\frac{\partial^+ \mathbf{h}_t}{\partial \theta} = \sum_{\tau=0}^{t-1} \frac{\partial^+ \mathbf{h}_t}{\partial \mathbf{h}_{t-\tau}} \frac{\partial \mathbf{h}_{t-\tau}}{\partial \theta} \quad (13)$$

because all partials $\frac{\partial \mathbf{x}_{t-\tau}}{\partial \theta}$ are $\mathbf{0}$.

⁴Note that the ordinary chain rule instead expresses $\frac{\partial^+ \mathbf{v}_i}{\partial \mathbf{v}_j}$ in terms of the *partial derivatives* that relate \mathbf{v}_i to all previous \mathbf{v}_k .

⁵This describes for example a linear layer + softmax + cross entropy loss, or a linear layer + l_2 loss, etc. Also note that this analysis is easily extended to the more general case where l_t is also a function of the shared parameters θ .

Table 1. Parameter counts (n_p), hidden unit counts (n_h), and optimal learning rates (α^*) for various task, method pairs.

	Copy ($D = 100$) $n_p \approx 46k$		Addition ($L = 100$) $n_p \approx 40k$		TIMIT $n_p \approx 49k$		Sequential pMNIST $n_p \approx 42k$	
	n_h	$\log_{10} \alpha^*$	n_h	$\log_{10} \alpha^*$	n_h	$\log_{10} \alpha^*$	n_h	$\log_{10} \alpha^*$
Simple RNN	203	-2.12 ± 0.11	201	-2.43 ± 0.20	197	-1.09 ± 0.25	198	-2.27 ± 0.10
LSTM	100	-1.55 ± 0.32	100	-1.85 ± 0.07	100	-0.63 ± 0.06	100	-1.11 ± 0.11
GRU	116	-1.23 ± 0.57	115	-1.97 ± 0.20	115	-0.95 ± 0.22	115	-0.98 ± 0.18
MIST	141	-1.47 ± 0.66	139	-2.31 ± 0.31	139	-0.91 ± 0.16	139	-1.35 ± 0.08

This simple decomposition, which extends the result from (Pascanu et al., 2013) to general NARX RNNs, breaks $\frac{\partial^+ \mathbf{h}_t}{\partial \theta}$ into its temporal components, making it clear that the spectral norm of $\frac{\partial^+ \mathbf{h}_t}{\partial \mathbf{h}_{t-\tau}}$ plays a major role in how $\mathbf{h}_{t-\tau}$ affects the final gradient $\frac{\partial^+ \mathbf{h}_t}{\partial \theta}$. In particular, if the norm of $\frac{\partial^+ \mathbf{h}_t}{\partial \mathbf{h}_{t-\tau}}$ is extremely small, then $\mathbf{h}_{t-\tau}$ has only a negligible effect on the final gradient, which in turn makes it extremely difficult to learn from events that occurred at $t - \tau$.

3.4. Gradient Components as Paths

Here we will apply Equation 10 repeatedly to associate gradient components with paths connecting $t - \tau$ to t , beginning with Equation 13 and handling simple RNNs and simple NARX RNNs in order. Applying Equation 10 to expand $\frac{\partial^+ \mathbf{h}_t}{\partial \mathbf{h}_{t-\tau}}$, we obtain

$$\frac{\partial^+ \mathbf{h}_t}{\partial \mathbf{h}_{t-\tau}} = \sum_{t \geq t' > t-\tau} \frac{\partial^+ \mathbf{h}_t}{\partial \mathbf{h}_{t'}} \frac{\partial \mathbf{h}_{t'}}{\partial \mathbf{h}_{t-\tau}} \quad (14)$$

3.4.1. SIMPLE RNNs

For simple RNNs, by examining Equation 2, we can immediately see that all partials $\frac{\partial \mathbf{h}_{t'}}{\partial \mathbf{h}_{t-\tau}}$ are $\mathbf{0}$ except for the one satisfying $t' = t - \tau + 1$. This yields

$$\frac{\partial^+ \mathbf{h}_t}{\partial \mathbf{h}_{t-\tau}} = \frac{\partial^+ \mathbf{h}_t}{\partial \mathbf{h}_{t-\tau+1}} \frac{\partial \mathbf{h}_{t-\tau+1}}{\partial \mathbf{h}_{t-\tau}} \quad (15)$$

Now, by applying Equation 10 again to $\frac{\partial^+ \mathbf{h}_t}{\partial \mathbf{h}_{t-\tau+1}}$, and then to $\frac{\partial^+ \mathbf{h}_t}{\partial \mathbf{h}_{t-\tau+2}}$, and so on, we trace out a path from $t - \tau$ to t , as shown in Figure 2(a), finally resulting the single term

$$\frac{\partial \mathbf{h}_t}{\partial \mathbf{h}_{t-1}} \dots \frac{\partial \mathbf{h}_{t-\tau+2}}{\partial \mathbf{h}_{t-\tau+1}} \frac{\partial \mathbf{h}_{t-\tau+1}}{\partial \mathbf{h}_{t-\tau}} \quad (16)$$

which is associated with the *only* path from $t - \tau$ to t , with one factor for each edge that is encountered along the path.

3.4.2. SIMPLE NARX RNNs

Next we consider simple NARX RNNs, again by expanding Equation 14. From Equation 8, we can see that up to

n_d partials are now nonzero, and that any particular partial $\frac{\partial \mathbf{h}_{t'}}{\partial \mathbf{h}_{t-\tau}}$ is nonzero if and only if $t' > t - \tau$ and t' and $t - \tau$ share an edge. Collecting these t' as the set $V_{t-\tau} = \{t' : t' > t - \tau \text{ and } (t - \tau, t') \in E\}$, we can write

$$\frac{\partial^+ \mathbf{h}_t}{\partial \mathbf{h}_{t-\tau}} = \sum_{t' \in V_{t-\tau}} \frac{\partial^+ \mathbf{h}_t}{\partial \mathbf{h}_{t'}} \frac{\partial \mathbf{h}_{t'}}{\partial \mathbf{h}_{t-\tau}} \quad (17)$$

We can then apply this exact same process to each $\frac{\partial^+ \mathbf{h}_t}{\partial \mathbf{h}_{t'}}$; by defining $V_{t'} = \{t'' : t'' > t' \text{ and } (t', t'') \in E\}$ for all t' , we can write

$$\frac{\partial^+ \mathbf{h}_t}{\partial \mathbf{h}_{t-\tau}} = \sum_{t' \in V_{t-\tau}} \sum_{t'' \in V_{t'}} \frac{\partial^+ \mathbf{h}_t}{\partial \mathbf{h}_{t''}} \frac{\partial \mathbf{h}_{t''}}{\partial \mathbf{h}_{t'}} \frac{\partial \mathbf{h}_{t'}}{\partial \mathbf{h}_{t-\tau}} \quad (18)$$

By continuing this process until only partials remain, we obtain a summation over all possible paths from $t - \tau$ to t . Each term in the sum is a product over factors, one per edge:

$$\frac{\partial \mathbf{h}_t}{\partial \mathbf{h}_{t'' \dots}} \dots \frac{\partial \mathbf{h}_{t''}}{\partial \mathbf{h}_{t'}} \frac{\partial \mathbf{h}_{t'}}{\partial \mathbf{h}_{t-\tau}} \quad (19)$$

3.4.3. DISCUSSION

First we note that this analysis extends easily to general NARX RNNs: the situation is the same as that of simple NARX RNNs, but with different sets of edges.

In all cases, we can bound the spectral norm of each term in the summation, one term per path. In particular,

$$\left\| \frac{\partial \mathbf{h}_t}{\partial \mathbf{h}_{t'' \dots}} \dots \frac{\partial \mathbf{h}_{t''}}{\partial \mathbf{h}_{t'}} \right\| \leq \left\| \frac{\partial \mathbf{h}_t}{\partial \mathbf{h}_{t'' \dots}} \right\| \dots \left\| \frac{\partial \mathbf{h}_{t''}}{\partial \mathbf{h}_{t'}} \right\| \leq \lambda^{n_e} \quad (20)$$

where λ is the maximum spectral norm of any individual factor and n_e is the number of edges on the path.

All terms with $\lambda < 1$ vanish⁶ exponentially fast, and in this paper we focus on worst-case behavior, where *all* terms

⁶We remark that if we instead let λ be the *minimum* norm and reverse the inequality in Equation 20, then we see that any term satisfying $\lambda > 1$ *explodes* exponentially fast. However in practice this behavior is often overcome with gradient clipping.

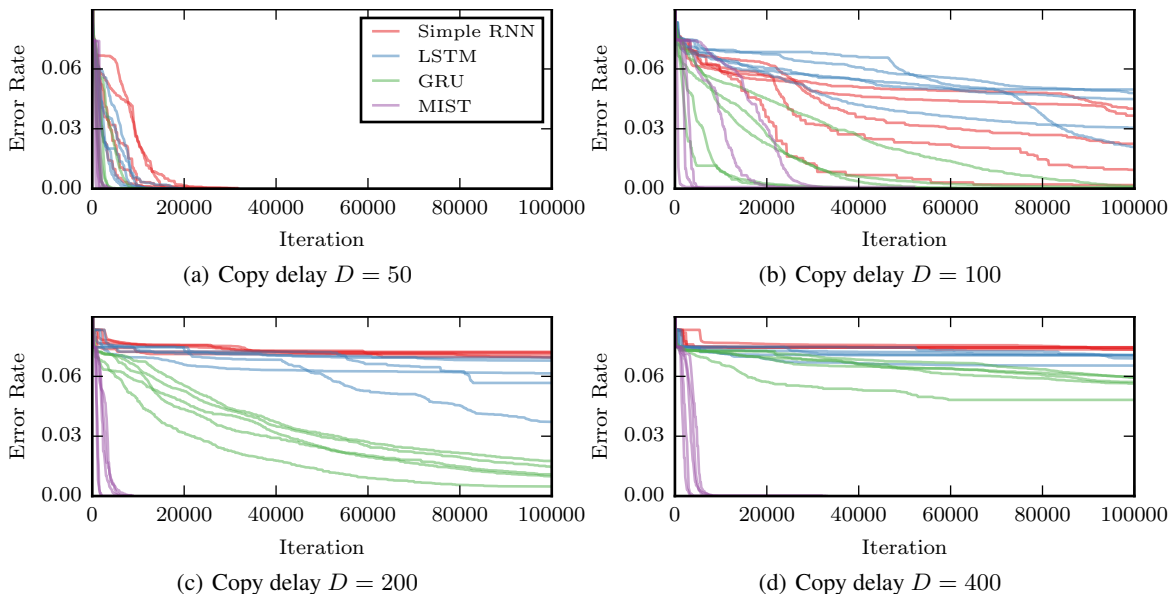


Figure 3. Validation curves for the copy problem. At each point, the error rate is computed using the entire validation set. For each method, the top 5 randomized trials out of 50 are shown (ranked according to final validation error). Note that in all cases, the simplest baseline – always predicting the *blank* symbol – yields an error rate of 0.083.

have $\lambda < 1$. In this scenario, we have a summation over vanishing terms, and terms corresponding to shorter paths vanish less quickly because λ^{n_e} goes to 0 quickly with n_e ; these shorter paths therefore dominate the sum.

Simple RNNs have a single path with $n_e = \tau$ while simple NARX RNNs have shortest paths with $n_e = \tau/n_d$, as shown in Figure 2.

4. Mixed History Recurrent Neural Networks

Compared to simple RNNs, simple NARX RNNs have both disadvantages and advantages: in Section 2, we saw that they increase computation by a factor of n_d ; and in the last section, we saw that simple NARX RNNs reduce the exponent of worst-case exponential decay from τ to τ/n_d . Is it possible to construct NARX RNNs which do not substantially increase computation and which address worst-case decay further?

In this section we introduce one such architecture, which we call MIXed hiSTory RNNs, described by

$$\mathbf{a}_t = \text{softmax}(\mathbf{W}_{ah}\mathbf{h}_{t-1} + \mathbf{W}_{ax}\mathbf{x}_t + \mathbf{b}_a) \quad (21)$$

$$\mathbf{r}_t = \sigma(\mathbf{W}_{rh}\mathbf{h}_{t-1} + \mathbf{W}_{rx}\mathbf{x}_t + \mathbf{b}_r) \quad (22)$$

$$\mathbf{h}_t = \tanh\left(\mathbf{W}_h\left[\mathbf{r}_t \odot \sum_{i=0}^{n_d-1} a_{ti}\mathbf{h}_{t-2^i}\right] + \mathbf{W}_x\mathbf{x}_t + \mathbf{b}\right) \quad (23)$$

Here, \mathbf{a}_t is a learned vector of coefficients which sum to 1, and \mathbf{r}_t is a reset gate, which we adopt from GRUs. At

each time step, a convex combination of delayed states is formed according to \mathbf{a}_t ; components of this combination are reset according to \mathbf{r}_t ; and finally the typical linear layer and nonlinearity are applied.

One key issue with simple NARX RNNs is that the exponent of the worst-case decay is reduced by only a factor of n_d . By using exponential delays, for any $\tau \leq 2^{n_d-1}$, a shortest-path exists with at most $\log \tau$ edges, thus reducing the worst-case exponent to $\log \tau$. (To see this, note that we can take steps of 1, 2, 4, \dots , 2^{n_d-1} , thus letting us reduce our distance to t by a factor of 2 at each step.)

A second key issue with simple NARX RNNs is that computation is increased by a factor of n_d . Here, by using a convex combination of delays, we avoid n_d separate state-to-state matrix-vector multiplications, thus eliminating this factor and yielding a computation count which is very similar to LSTM and GRUs. In particular, we require 3 such matrix-vector multiplies in comparison to 3 in the case of GRUs and 4 in the case of LSTM. (We also require an additional $n_d \cdot n_h$ multiplications for the convex combination, but this is negligible in comparison to the n_h^2 multiplications for each matrix-vector multiplication, as $n_h \gg n_d$.)

5. Experiments

Here we describe a set of large-scale experiments to compare simple RNNs, LSTM, GRUs, and MIST RNNs. We will release code for all methods and experiments, including data generation and preprocessing.

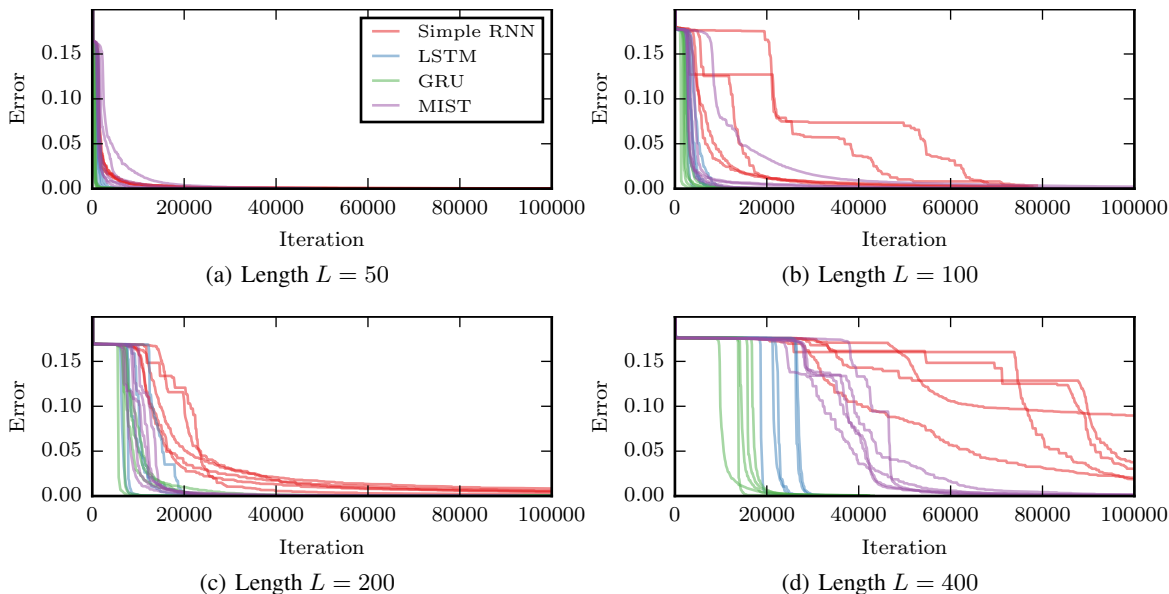


Figure 4. Validation curves for the addition problem. At each point, the error is computed using the entire validation set. For each method, the top 5 randomized trials out of 50 are shown (ranked according to final validation error). Note that the simplest baseline – always predicting 1.0 – yields an error of 0.167.

We remark that the copy problem, addition problem, and sequential pMNIST task were all chosen because they are commonly used to test an RNN’s ability to capture long-term dependencies (Hochreiter & Schmidhuber, 1997; Martens & Sutskever, 2011; Le et al., 2015; Arjovsky et al., 2016; Henaff et al., 2016; Danihelka et al., 2016).

We emphasize that these experiments intend to evaluate MIST RNNs in isolation, as their approach to tackling the vanishing is *orthogonal* to LSTM and GRUs. Other state of the art techniques such as batch normalization (Cooijmans et al., 2016), layer normalization (Ba et al., 2016), and zoneout (Krueger et al., 2016) are applicable to all methods involved, and such enhancements are left for future work.

5.1. Experimental Setup

To aid reproducibility, we maintain as much consistency as possible between experiments. The baseline for all tasks is LSTM⁷ with a single layer of 100 hidden units. We also use one hidden layer with all other methods, and the number of hidden units is chosen so that the number of parameters in the model is as close as possible to that of LSTM. For MIST RNNs, we use delays 1, 2, 4, \dots , 128. All weight matrices are initialized using a normal distribution with a mean of 0 and a standard deviation of $1/\sqrt{n_h}$, where n_h is the number of hidden units. For optimization, stochastic

⁷The term LSTM is often overloaded; we use the variant with forget gates and without peephole connections, which performs similarly to more complex variants (Greff et al., 2016).

gradient descent is used with a momentum of 0.9, with gradient clipping⁸ as described by (Pascanu et al., 2013) at 1, and with a minibatch size of 100.

Biases are generally initialized to 0, but we follow best practice for LSTM by initializing the forget-gate bias to 1 (Gers et al., 2000; Jozefowicz et al., 2015) and for GRUs by initializing the update-gate bias to 1. This encourages both forward flow and backward flow early on in training.

As in most deep-learning experiments, the learning rate is a crucial hyperparameter (Bengio, 2012), and in addition has been found to account for the majority of performance variability in previous large-scale LSTM experiments (Greff et al., 2016). To ensure fair comparisons, we avoid manual learning-rate tuning in its entirety, and instead run 50 trials for each experimental configuration. In each trial, the learning rate is drawn uniformly at random in log space between 10^{-4} and 10^1 , and initial weight matrices are also redrawn at random. We report results over the top 10% of trials according to validation-set error⁹. Table 1 summarizes the number of hidden units and the optimal learning rates for various task, method pairs.

⁸The term *gradient scaling* is more appropriate here, since this is precisely what occurs when the global norm over gradients exceeds some threshold. We use the term gradient clipping to maintain consistency with literature.

⁹An alternative option is to report results over *all* trials. However, because the majority of trials yields bad performance for all methods, this simply blurs comparisons. See for example Figure 3 of (Greff et al., 2016), which compares these two options.

5.2. The Copy Problem

The copy problem is a synthetic task that explicitly challenges a network to store and reproduce information from the past. Our setup follows (Arjovsky et al., 2016), which is in turn based on (Hochreiter & Schmidhuber, 1997). An input sequence begins with L relevant symbols to be copied, is followed by a delay of $D - 1$ special blank symbols and 1 special go symbol, and ends with L additional blank symbols. The corresponding target sequence begins with $L + D$ blank symbols and ends with a copy of the relevant symbols from the inputs (in the same order).

In our experiments, the L relevant symbols are drawn at random (with replacement) from the set $\{0, 1, \dots, 9\}$; D is always a multiple of 10; and L is chosen to be $D/10$. This way the simplest baseline of always predicting the blank symbol yields a constant error rate for all experiments. No input preprocessing of any kind is performed.

We run experiments with copy delays of $D = 50, 100, 200,$ and 400 . In each case, we generate 100,000 examples for training and 1,000 examples for validation. Training is carried out by minimizing cross-entropy loss.

Results are shown in Figure 3. With a short copy delay of $D = 50$, we can see that all methods, even simple RNNs, can solve the task in a reasonable amount of time. However, as the copy delay D is increased, we can see that simple RNNs, LSTM, and GRUs become unable to learn a solution, whereas MIST RNNs are relatively unaffected. We also note that our LSTM results are consistent with (Arjovsky et al., 2016; Henaff et al., 2016). Finally we note that it is known that orthogonal-weight-matrix based approaches are particularly well suited to this problem (Henaff et al., 2016). MIST RNNs, *without* using such initializations, perform similarly to such approaches (Arjovsky et al., 2016; Henaff et al., 2016).

5.3. The Addition Problem

The addition problem is a synthetic task that challenges a network to add two marked numbers from a long sequence. Our setup follows (Arjovsky et al., 2016; Henaff et al., 2016), which is in turn based on (Hochreiter & Schmidhuber, 1997). A length- L input sequence consists of L 2-D vectors, with each vector \mathbf{x}_t having its first element drawn from a uniform distribution over $[0, 1]$ and its second element being either 0 or 1. The second element of nearly all input vectors is 0, with the exception of two, one chosen from the first half of the sequence and one chosen from the second. The positions of the two 1s mark the numbers to add and are chosen randomly. The target is then the sum of the two marked numbers. The simplest baseline of always predicting 1.0 yields an expected sum-of-squares error of $\frac{1}{6}$. No input preprocessing of any kind is performed.

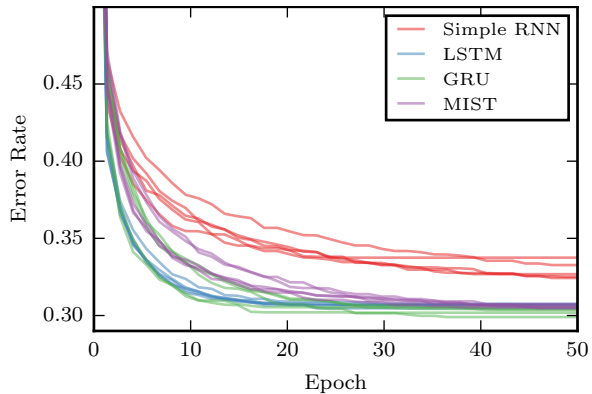


Figure 5. Validation curves for TIMIT phoneme recognition. At each point, the error rate is computed using the entire validation set. For each method, the top 5 randomized trials out of 50 are shown (ranked according to final validation error).

Table 2. Test-set error rates for TIMIT phoneme recognition. Means and standard deviations are computed using the top 5 randomized trials out of 50 (ranked according to performance on the validation set). Welch’s t -test at a significance level of 0.05 suggests that there is no significant difference among LSTM, GRU, and MIST, and that all of these methods are significantly different from simple RNNs.

	Error Rate (%)
Simple RNN	34.1 ± 0.3
LSTM	32.1 ± 0.2
GRU	31.7 ± 0.4
MIST	32.0 ± 0.3

We run experiments with lengths $L = 50, 100, 200,$ and 400 . In each case, we generate 100,000 examples for training and 1,000 examples for validation. Training is carried out by minimizing sum-of-squares error.

Results are shown in Figure 4. Surprisingly all methods, including simple RNNs, learn to (approximately) solve this problem, even with large sequence lengths. However here LSTM and GRUs converge more rapidly than MIST RNNs.

5.4. TIMIT Phoneme Recognition

Here we consider the task of framewise phoneme recognition using the TIMIT corpus (Garofolo et al., 1993). Each frame is originally labeled as 1 of 61 different phonemes. We follow common practice and collapse these into a smaller set of 39 phonemes (Lee & Hon, 1989), and we include glottal stops to yield 40 classes in total. We follow (Greff et al., 2016) and extract 12 mel frequency cepstral coefficients plus energy every 10ms using 25ms Hamming windows and a pre-emphasis coefficient of 0.97. However we do not use derivatives, resulting in 13 inputs per frame.

Each input sequence is individually shifted and scaled to have mean 0 and variance 1 over each dimension.

We form our splits according to (Halberstadt, 1998), resulting in 3696 sequences for training, 400 sequences for validation, and 192 sequences for testing. Training is carried out by minimizing cross-entropy loss.

Validation curves are shown in Figure 5 and final test error rates are shown in Table 2. Here we can see that LSTM, GRUs, and MIST RNNs all yield very similar performance, and that all of these methods outperform simple RNNs. We remark that our results cannot be directly compared to those in (Greff et al., 2016). First, for consistency with other experiments, we use unidirectional RNNs, which make predictions based only on past inputs; (Greff et al., 2016) use bidirectional LSTM. Second, (Greff et al., 2016) uses the full set of 61 phonemes.

5.5. Sequential pMNIST Classification

The sequential MNIST task (Le et al., 2015) consists of classifying 28x28 MNIST images (LeCun et al., 1998) as one of 10 digits, by scanning pixel by pixel – left to right, top to bottom – and emitting a label upon completion. Sequential pMNIST (Le et al., 2015) is a challenging variant where a random permutation of pixels is chosen and applied to all images before classification. This reduces the locality of image patterns and increases the need for solutions to rely on long-term dependencies. Data preprocessing is kept minimal, with each input image individually shifted and scaled to have mean 0 and variance 1.

We split the official training set into two parts, the first 58,000 used for training and the last 2,000 used for validation. Our test set is the same as the official test set, consisting of 10,000 images. Training is carried out by minimizing cross-entropy loss.

Validation curves are shown in Figure 6 and final test error rates are shown in Table 3. Here, MIST RNNs significantly outperform all other methods. We also remark that our LSTM error rates are consistent with best previously-reported values, such as the error rates of 9.8% in (Cooijmans et al., 2016) and 12% in (Arjovsky et al., 2016).

Finally we remark that previous work suggest that simple RNNs fail entirely on this task (Le et al., 2015), whereas in our experiments simple RNNs obtain a reasonable error rate of about 13%. This discrepancy may be due to our finer learning-rate search.

6. Conclusions

In this work we analyzed the vanishing gradient problem for NARX RNNs, which provided motivation for NARX RNNs with exponential delays and the efficient variant in-

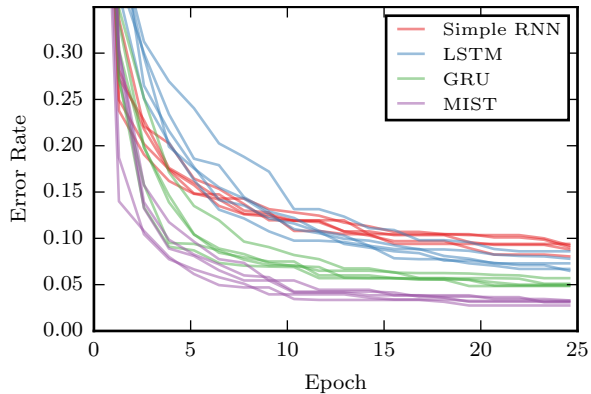


Figure 6. Validation curves for sequential pMNIST classification. At each point, the error rate is computed using the entire validation set. For each method, the top 5 randomized trials out of 50 are shown (ranked according to final validation error).

Table 3. Test-set error rates for sequential pMNIST classification. Means and standard deviations are computed using the top 5 randomized trials out of 50 (ranked according to performance on the validation set). Welch’s t -test at a significance level of 0.05 suggests that there is a significant difference between all methods.

	Error Rate (%)
Simple RNN	12.9 ± 0.8
LSTM	10.4 ± 0.7
GRU	7.7 ± 0.2
MIST	5.5 ± 0.2

roduced in this paper, MIST RNNs. In particular, we saw that for $\tau \leq 2^{n_d-1}$, MIST RNNs reduce the decay’s worst-case exponent from τ/n_d to $\log \tau$, while maintaining computational complexity that is similar to LSTM and GRUs.

Experiments across 4 diverse tasks showed that MIST RNNs are competitive with LSTM and GRUs for capturing long-term dependencies, and in some cases outperformed both LSTM and GRUs. We are excited by these results because the approach is *orthogonal* to that taken by LSTM and GRUs. In future work, it will be interesting to see if *combining* the two mechanisms can improve results further, by capturing the respective benefits of both approaches.

Acknowledgments

This work was supported by the National Institutes of Health (1R01-DE025265) and by the Institute for Advanced Study at Technische Universität München. We are also grateful to the Maryland Advanced Research Computing Center, which was used extensively to conduct the experiments in this work.

References

- Arjovsky, Martin, Amar, Shah, and Bengio, Yoshua. Unitary evolution recurrent neural networks. *International Conference on Machine Learning (ICML)*, 2016.
- Ba, Jimmy Lei, Kiros, Jamie Ryan, and Hinton, Geoffrey E. Layer normalization. *arXiv preprint arXiv:1607.06450*, 2016.
- Bahdanau, Dzmitry, Cho, KyungHyun, and Bengio, Yoshua. Neural machine translation by jointly learning to align and translate. *International Conference on Learning Representations (ICLR)*, 2015.
- Bengio, Yoshua. Practical recommendations for gradient-based training of deep architectures. *Neural networks: Tricks of the trade*, 2012.
- Bengio, Yoshua, Simard, Patrice, and Frasconi, Paolo. Learning long-term dependencies with gradient descent is difficult. *IEEE Transactions on Neural Networks*, 5(2):157–166, 1994.
- Cho, Kyunghyun, van Merriënboer, Bart, Gülçehre, Çağlar, Bahdanau, Dzmitry, Bougares, Fethi, Schwenk, Holger, and Bengio, Yoshua. Learning phrase representations using rnn encoder–decoder for statistical machine translation. *Proceedings of the 2014 Conference on Empirical Methods in Natural Language Processing (EMNLP)*, 2014.
- Cooijmans, Tim, Ballas, Nicolas, Laurent, César, and Courville, Aaron. Recurrent batch normalization. *arXiv preprint arXiv:1603.09025*, 2016.
- Danihelka, Ivo, Wayne, Greg, Uria, Benigno, Kalchbrenner, Nal, and Graves, Alex. Associative long short-term memory. *International Conference on Machine Learning (ICML)*, 2016.
- El Hahi, Salah and Bengio, Yoshua. Hierarchical recurrent neural networks for long-term dependencies. *Advances in neural information processing systems (NIPS)*, 1995.
- Elman, Jeffrey L. Finding structure in time. *Cognitive science*, 14(2):179–211, 1990.
- Garofolo, John S, Lamel, Lori F, Fisher, William M, Fiscus, Jonathon G, and Pallett, David S. DARPA TIMIT acoustic-phonetic continuous speech corpus CD-ROM. NIST speech disc 1-1.1. *NASA STI/Recon technical report*, 1993.
- Gers, Felix A, Schmidhuber, Jürgen, and Cummins, Fred. Learning to forget: Continual prediction with LSTM. *Neural computation*, 12(10):2451–2471, 2000.
- Graves, Alex, Wayne, Greg, and Danihelka, Ivo. Neural Turing machines. *arXiv preprint arXiv:1410.5401*, 2014.
- Greff, K., Srivastava, R. K., Koutník, J., Steunebrink, B. R., and Schmidhuber, J. LSTM: A search space odyssey. *IEEE Transactions on Neural Networks and Learning Systems*, 2016.
- Halberstadt, Andrew K. *Heterogeneous acoustic measurements and multiple classifiers for speech recognition*. PhD thesis, Massachusetts Institute of Technology, 1998.
- Henaff, Mikael, Szlam, Arthur, and LeCun, Yann. Orthogonal RNNs and long-memory tasks. *International Conference on Machine Learning (ICML)*, 2016.
- Hochreiter, Sepp. Untersuchungen zu dynamischen neuronalen netzen. *Diploma, Technische Universität München*, pp. 91, 1991.
- Hochreiter, Sepp and Schmidhuber, Jürgen. Long short-term memory. *Neural computation*, 9(8):1735–1780, 1997.
- Jozefowicz, Rafal, Zaremba, Wojciech, and Sutskever, Ilya. An empirical exploration of recurrent network architectures. *International Conference on Machine Learning (ICML)*, 2015.
- Koutník, Jan, Greff, Klaus, Gomez, Faustino, and Schmidhuber, Jürgen. A clockwork RNN. *International Conference on Machine Learning (ICML)*, pp. 1863–1871, 2014.
- Krueger, David, Maharaj, Tegan, Kramár, János, Pezeshki, Mohammad, Ballas, Nicolas, Ke, Nan Rosemary, Goyal, Anirudh, Bengio, Yoshua, Larochelle, Hugo, Courville, Aaron, et al. Zoneout: Regularizing rnns by randomly preserving hidden activations. *arXiv preprint arXiv:1606.01305*, 2016.
- Le, Quoc V, Jaitly, Navdeep, and Hinton, Geoffrey E. A simple way to initialize recurrent networks of rectified linear units. *arXiv preprint arXiv:1504.00941*, 2015.
- LeCun, Yann, Bottou, Léon, Bengio, Yoshua, and Haffner, Patrick. Gradient-based learning applied to document recognition. *Proceedings of the IEEE*, 86(11):2278–2324, 1998.
- Lee, K-F and Hon, H-W. Speaker-independent phone recognition using hidden Markov models. *IEEE Transactions on Acoustics, Speech, and Signal Processing*, 37(11):1641–1648, 1989.
- Lin, Tsungnan, Horne, Bill G, Tino, Peter, and Giles, C Lee. Learning long-term dependencies in NARX recurrent neural networks. *IEEE Transactions on Neural Networks*, 7(6):1329–1338, 1996.

- Martens, James and Sutskever, Ilya. Learning recurrent neural networks with hessian-free optimization. In *International Conference on Machine Learning (ICML)*, 2011.
- Miao, Yajie, Gowayyed, Mohammad, and Metze, Florian. EESEN: End-to-end speech recognition using deep RNN models and WFST-based decoding. *Automatic Speech Recognition and Understanding (ASRU)*, pp. 167–174, 2015.
- Oord, Aaron Van den, Kalchbrenner, Nal, and Kavukcuoglu, Koray. Pixel recurrent neural networks. *International Conference on Machine Learning (ICML)*, 2016.
- Pascanu, Razvan, Mikolov, Tomas, and Bengio, Yoshua. On the difficulty of training recurrent neural networks. *International Conference on Machine Learning (ICML)*, 28:1310–1318, 2013.
- Plate, Tony A. Holographic recurrent networks. *Advances in neural information processing systems (NIPS)*, 1993.
- Rumelhart, David E, Hinton, Geoffrey E, and Williams, Ronald J. Learning representations by back-propagating errors. *Nature*, 323(6088):533–538, 1986.
- Sukhbaatar, Sainbayar, Weston, Jason, Fergus, Rob, et al. End-to-end memory networks. *Advances in neural information processing systems (NIPS)*, 2015.
- Werbos, Paul J. Generalization of backpropagation with application to a recurrent gas market model. *Neural networks*, 1(4):339–356, 1988.
- Werbos, Paul J. Maximizing long-term gas industry profits in two minutes in lotus using neural network methods. *IEEE Transactions on Systems, Man, and Cybernetics*, 19(2):315–333, 1989.
- Werbos, Paul J. Backpropagation through time: what it does and how to do it. *Proceedings of the IEEE*, 78(10): 1550–1560, 1990.
- Weston, Jason, Chopra, Sumit, and Bordes, Antoine. Memory networks. *International Conference on Learning Representations (ICLR)*, 2015.
- Williams, Ronald J and Zipser, David. A learning algorithm for continually running fully recurrent neural networks. *Neural computation*, 1(2):270–280, 1989.
- Wu, Yonghui, Schuster, Mike, Chen, Zhifeng, Le, Quoc V, Norouzi, Mohammad, Macherey, Wolfgang, Krikun, Maxim, Cao, Yuan, Gao, Qin, Macherey, Klaus, et al. Google’s neural machine translation system: Bridging the gap between human and machine translation. *arXiv preprint arXiv:1609.08144*, 2016.